Since the voltages, V_{ds3} and V_{ds4}, across M_3 and M_4 are 0 V at t_1, M_3 and M_4 can be turned on with ZVS. Moreover, since i_L compensates a large portion of the plasma discharge current I_{dis} during this period, the plasma discharge current flowing through M_3 and M_4 are considerably reduced as shown in Fig. 2b. Therefore, the voltage drops across power switches are not serious and wall charges are well accumulated. Since C_p is connected between GND and V_s through M_3 and M_4, the voltage v_{Cp} is maintained to $-V_s$. The circuit operation of t_2–t_4 is similar to that of t_0–t_2.

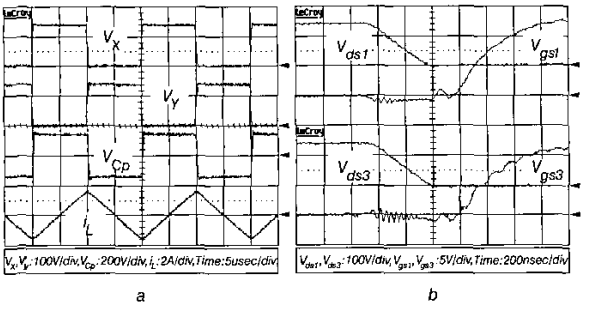

Fig. 3 *Experimental waveforms of proposed circuit (in displaying the white image)*

a Voltage waveforms across *X*, *Y*, and PDP and current waveform through *L*
b Turn on transients of M_1 and M_3

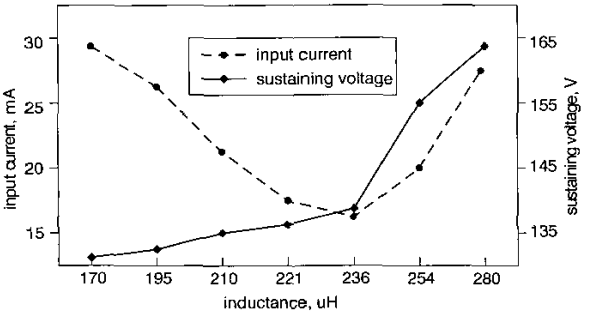

Fig. 4 *Measured input current and sustaining voltage according to L*

Design considerations: Since the brightness of a PDP increases with the frequency, the rising times are required to be as short as possible. Therefore, in application, the PDP usually works at a high frequency such as from 50 to 250 kHz. The interval t_0–t_1 (or t_2–t_3) is the desired rising time, and C_p and C_{oss} are as known values. Thus, the value of L can be determined from (1) as follows:

$$L = \frac{T_S(t_1 - t_0) - 2(t_1 - t_0)^2}{16(C_p + C_{oss})} \quad (2)$$

Experimental results and discussions: The prototype ERC for a PDP is implemented with specifications of $L = 236$ uH, $C_p = 2$ nF (6 inch PDP), gate driver $IC = IR2110$, $M_1 = M_2 = M_3 = M_4 = 2SK2995$, switching frequency = 50 kHz, and $V_s = 140$ V. Fig. 3 shows the experimental waveforms of the proposed circuit, when the white image is displayed. As can be seen in Fig. 3*a*, a current source built in the inductor completely charges C_p to V_s or $-V_s$ with no voltage notch. This is because inductor currents compensate the large amount of plasma discharge current. Therefore, the current through power switches is considerably lowered and the voltage drops across the switches are favourably reduced, which will attract more wall charge to deposit on the dielectric layer of the electrodes, i.e. the wall voltage is larger, and it helps to maintain the panel to light at lower voltage such as 140 V compared with about 165 V for a prior circuit. Fig. 3*b* shows that M_1 and M_3 are turned on with ZVS after V_{ds1} and V_{ds3} drop to 0 V. M_2 and M_4 are also turned on with ZVS. Fig. 4 shows that the smaller inductor can maintain the panel to display the white image at the lower sustaining voltage with more effect of the discharge current compensation. As can be seen in Table 1, the number of devices used in the proposed circuit is less than the prior circuit due to the absence of the auxiliary circuit. Therefore, it features a simpler structure, less mass, and lower cost of production.

Table 1: Number of devices for 6 inch PDP

		Prior circuit	Proposed circuit
Switch	M_1, M_4	2SK2995:2(EA)	2SK2995:2(EA)
	M_2, M_3	2SK2995:2(EA)	2SK2995:2(EA)
	Auxiliary circuit	IRFP250:8(EA)	0(EA)
Energy-recovery inductor: L		8.1uH:2(EA)	236 uH:2(EA)
Diode		F10KF40:8(EA)	0(EA)
Gate driver IC		IR2110:6(EA)	IR2110:2(EA)
Energy-recovery capacitor: C_a		2.2 uF/150 V:4(EA)	1uF/150V:2(EA)

Conclusion: A new current-fed ERC has been presented to overcome the drawbacks of the prior circuit. It features a simpler structure, less mass, fewer devices, and lower cost of production. Furthermore, since all four switches are turned on with ZVS, it has a higher efficiency and lower EMI. In particular, since it compensates the plasma discharge current, it enables the panel to light at a lower voltage than the prior circuit. Therefore, this proposed circuit is expected to be well suited for hang-on-the-wall TVs.

Acknowledgment: This work was supported by the Institute of Information Technology Assessment.

24 March 2003
Electronics Letters Online No: 20030702
DOI: 10.1049/el:20030702

Sang-Kyoo Han, Gun-Woo Moon and Myung-Joong Youn (*Department of Electrical Engineering, Korea Advanced Institute of Science and Technology, 373-1, Gusong-Dong, Yusong-Gu, Daejeon, 305-701, Republic of Korea*)

E-mail: mmyoun@ee.kaist.ac.kr

References

1 WEBER, L.F., and WOOD, M.B.: 'Energy recovery sustain circuit for the AC plasma display'. Proc. Symp. Society for Information Display, 1987, pp. 92–95
2 LIU, C.-C., HSU, H.-B., LO, S.-T., and CHEN, C.-L.: 'An energy-recovery sustaining driver with discharge current compensation for AC plasma display panel', *IEEE Trans. Ind. Electron.*, 2001, **48**, (2), pp. 344–351

Vibration reduction of resonant structures using charge controlled piezoelectric actuators

B.J.G. Vautier and S.O.R. Moheimani

A new charge controller design for piezoelectric transducers attached to highly resonant flexible beams is presented that significantly dampens the structure and naturally reduces the negative effects of hysteresis. Experimental results demonstrating the effectiveness of this technique are included.

Introduction: Even though piezoelectric transducers offer excellent actuation and sensing capabilities, they suffer from hysteresis, which occurs when relatively high electric fields are applied to the piezoelectric transducer or the device is being operated under high strains.

Various methods have been proposed to model and compensate for this undesirable effect. Some of these include the Preisach hysteresis model for piezoelectric materials [1], the general Maxwell resistive capacitor model, the phaser approach, describing functions and the use of current or charge sources for the actuation. Each of these methods have their advantages and disadvantages.

In this Letter we will concentrate on the use of charge source, which has been shown to naturally minimise the effects of hysteresis [2] as

well as increase the gain and phase margins of the controlled system. By simply regulating the charge (or current) a fivefold reduction in hysteresis has been achieved. Recently improvements to the design of charge amplifiers have been presented by Fleming and Moheimani [3], which have enabled us to effectively implement a charge source to reduce hysteresis as well as a charge controller to regulate vibrations of highly resonant structures.

Charge controlled piezoelectric actuators: The structure under study comprises a pair of collocated piezoelectric (PZT) patches, which are securely attached to a cantilever Euler beam.

Numerous control schemes, such as LQG, H_∞, H_2 and the like, have successfully been implemented on similar structures (where voltage is used as the input signal). The controllers are designed to deal with system uncertainty and guarantee the stability of the feedback control system. They do not however explicitly reduce hysteresis. These uncertainty issues can be alleviated by using current or charge amplifiers to drive the actuator instead of voltage.

The input (charge) to output (voltage) relationship of the structure can be determined by looking at the electrical representation of a piezoelectric transducer (Fig. 1), noticing that each PZT patch is modelled as a capacitor in series with a strain dependent voltage source.

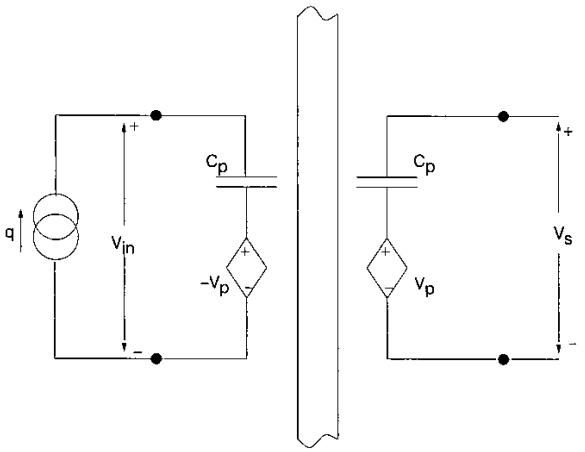

Fig. 1 *Collocated structure with charge source*

By writing the KVL around the left hand loop we get, $V_{in} = (1/C_p)q - V_p$. If we now define $G_{vv}(s)$ as $V_p(s)/V_{in}(s)$, we can determine that G_{vq} is equal to:

$$G_{vq} = \frac{V_p}{q} = \frac{1}{C_p}\left(\frac{G_{vv}}{1+G_{vv}}\right) \tag{1}$$

This result is interesting as it suggests that the poles of G_{vq} are different from the resonance frequencies of the structure (which are the poles of G_{vv}).

Based on the relationship between G_{vq} and G_{vv} given in (1) we will design a controller K_q, which will reject the disturbances w entering the system through a second piezoelectric patch as shown in Fig. 2. We will call $\tilde{G}_{vv}$ the transfer function from the voltage disturbance w to the output sensor voltage V_p (i.e. $\tilde{G}_{vv} = V_p/w$) measured in open loop.

We would like to point out that designing a controller based on G_{vq} could be misleading. To clarify this point, let us assume that a controller K_q has already been designed for the collocated system. We have already established that poles of G_{vq} are different from those of G_{vv}. Therefore, if a disturbance is entering the system, say through the voltage applied to a non-collocated piezoelectric actuator, as shown in Fig. 2, then the resulting closed loop transfer function from w to V_p will be $\tilde{G}_{vv}/(1+G_{vq}K_q)$ which is equivalent to $(\tilde{G}_{vv}(1+G_{vv}))/(1+(1+K_q/C_p)G_{vv})$.

Now, $\tilde{G}_{vv}$ and G_{vv} share similar poles, which is a property of flexible structures. It is, therefore, straightforward to observe that the closed loop transfer function of the last equation includes the open loop poles associated with G_{vv}. Hence, the controller K_q, if designed directly from G_{vq} is not adding any effective damping to the system.

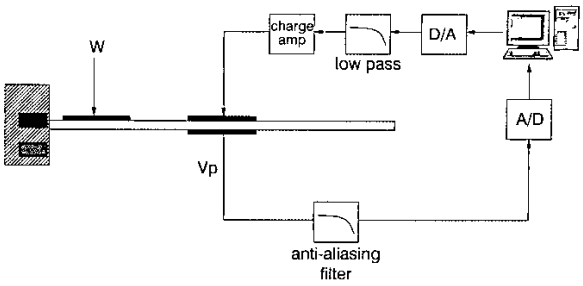

Fig. 2 *Closed loop with controller schematic*

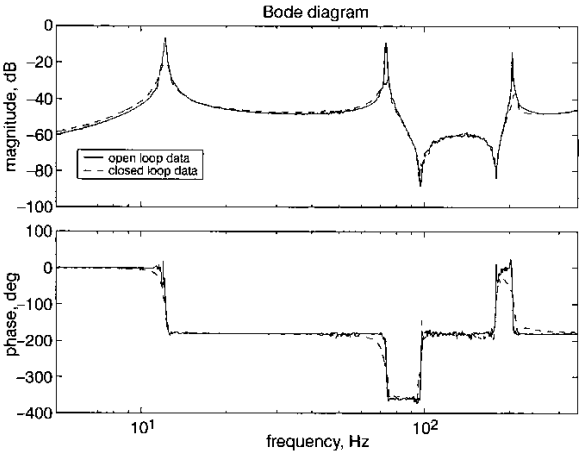

Fig. 3 *Measured open and closed loop frequency responses for input voltage disturbance w to output voltage V_p*

If we are to use a charge amplifier to regulate vibration of the beam, we need to make sure that the charge controller K_q will place the closed loop poles of this system at the same locations a voltage controller (K_v) would. In effect we need to enforce the following:

$$\frac{\tilde{G}_{vv}}{1+K_vG_{vv}} = \frac{\tilde{G}_{vv}}{1+K_qG_{vq}} \tag{2}$$

If we substitute (1) into (2) and rearrange it, we obtain:

$$K_q = C_pK_v(1+G_{vv}) \tag{3}$$

This suggests that to design an effective controller for the charge-driven system, we first need to calculate a controller K_v for the voltage driven system, which we then filter by $C_p(1+G_{vv})$.

Design of LQR controller: Based on these relationships we will design a charge controller to reduce vibrations of the beam. We designed a controller, with a cost function J that weighted the output voltage V_p and the input voltage V where $J = \int_0^\infty \{V_p'QV_p + V'RV\}\,dt$.

We made sure that extra damping was added to the structure by placing the poles of G_{vv} deeper into the left half of the complex plane.

Once the weightings Q and R were appropriately chosen, we built a pole placement observer to predict the states of the plant. This is necessary as we are only measuring the output voltage V_p across the sensor. Once we have obtained a suitable voltage controller K_v we can determine the charge controller K_q by using (3).

Experimental results: The results obtained with the K_q controller were very satisfactory. We measured the transfer function $\tilde{G}_{vv}$ (input disturbance to output voltage V_p) with and without the controller K_q. These are shown in Fig. 3. On average a 16 dB reduction was achieved for each mode.

We also measured the velocity step response at the tip of the beam (Fig. 4). The results indicate that the beam is significantly more damped by using the controller K_q.

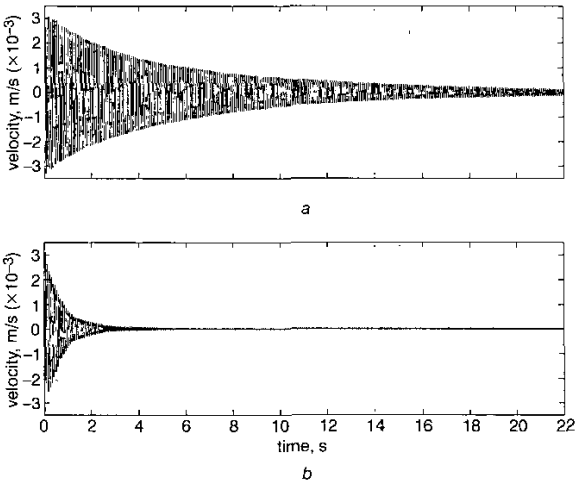

Fig. 4 *Step response at tip of beam*

a Step response without controller
b Step response with controller

Conclusion: Charge unlike voltage naturally reduces hysteresis in piezoelectric transducers. When designing a charge controller care must be taken to effectively dampen the structural vibrations of the system. A procedure to achieve this has been discussed in this Letter and has been shown to successfully reduce disturbance vibrations on a highly resonant beam.

3 April 2003
Electronics Letters Online No: 20030708
DOI: 10.1049/el:20030708

B.J.G. Vautier and S.O.R. Moheimani (*School of Electrical Engineering and Computer Science, The University of Newcastle, University Drive, Callaghan, NSW 2304, Australia*)

E-mail: bvautier@ee.newcastle.edu.au

References

1 MAYERGOYZ, I.: 'Mathematical models of hysteresis' (Springer-Verlag, 1991)
2 NEWCOMB, C.V., and FLINN, I.: 'Improving the linearity of piezoelectric ceramic actuators', *Electron. Lett.*, 1982, **18**, pp. 442–443
3 FLEMING, A.J., and MOHEIMANI, S.O.R.: 'Precision current and charge amplifiers for driving highly capacitive piezoelectric loads', *Electron. Lett.*, 2003, **39**, pp. 282–284

Addressing static and dynamic errors in unit element multibit DACs

J. De Maeyer, P. Rombouts and L. Weyten

Nonlinearity in multibit current-steering digital-to-analogue converters (DACs) originates from static mismatch and switching imperfections. Several techniques are presented to avoid this nonlinearity. When applied, the DACs are suitable for use in the feedback of continuous-time ΣΔ-converters.

Introduction: For high-speed applications continuous-time ΣΔ analogue-to-digital converters (ADCs) are more attractive than their discrete-time counterparts. They usually have a current-steering DAC in the feedback path. When a multibit variant is used, static mismatch and dynamic switching imperfections (e.g. turn-on and turn-off delay, rise time, ...) will limit the linearity of the converter [1]. In the past dynamic element matching techniques were presented to tackle static mismatch [2–4]. However, problems with dynamic errors were paid little attention. This Letter provides several implementations to tackle the problems with dynamic errors while avoiding performance degradation due to static error sources.

Dynamic error model: Consider a current-steering DAC consisting of N nominally matched current sources. A typical waveform for the ith element is shown in Fig. 1. Three deviations from the ideal output can be recognised. First, the sources exhibit static mismatch (ε_i). Secondly, switching is not ideal (e.g. nonzero rise time, ...). Thirdly, the switching imperfections differ from element to element. This is called dynamic mismatch. As in [1] our analysis will be performed in discrete-time and only the low frequency information will be considered. The grey-coloured surfaces of Fig. 1 correspond to the dynamic error of the current source. This error can be defined as to consist of two parts. One part δ is the mean value of the dynamic error over the N elements. The other part δ_i is caused by the variance in the dynamic error from element to element, i.e. dynamic mismatch. By definition the mean value of δ_i is zero.

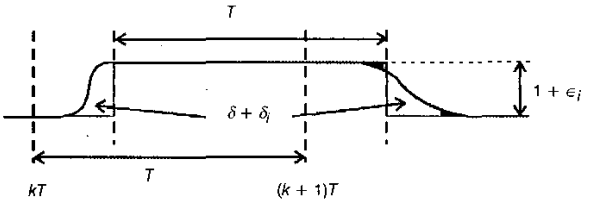

Fig. 1 *Typical output waveform of a current source*

T is clock period. Both grey-coloured regions represent the dynamic error and have an equal surface. The two black surfaces add in an opposite way to the total dynamic error

Let k indicate time and $D(k)$ be the input value of the DAC. For each element i a selection signal $S_i(k)$ is generated, in such a way that $D(k) = \sum_{i=1}^{N} S_i(k)$. Thus, $S_i(k)$ equals 1 if element i is used at point k in time, and 0 otherwise. Then, it can be derived that the total DAC error, referred to as $e(k)$, is given by:

$$e(k) = \underbrace{\sum_{i=1}^{N} \varepsilon_i S_i(k)}_{e_1(k)} + \underbrace{\delta \sum_{i=1}^{N} |S_i(k) - S_i(k-1)|}_{e_2(k)} + \underbrace{\sum_{i=1}^{N} \delta_i |S_i(k) - S_i(k-1)|}_{e_3(k)} \quad (1)$$

A similar model was used in [1], but there $e_3(k)$ was not taken into account.

The first error contribution $e_1(k)$ in (1) originates in the static mismatch ε_i between the current sources. By properly selecting $S_i(k)$, $e_1(k)$ can be spectrally shaped. The switching imperfections cause the second term $e_2(k)$ and dynamic mismatch the third term $e_3(k)$. They will only contribute to the total DAC error when elements are switched. Surprisingly this is independent of whether these elements are turned on or off. In general, $e_2(k)$ and $e_3(k)$ depend in a complex and nonlinear way on the input value $D(k)$. This causes distortion.

Tackling $e_2(k)$: As can be seen from (1), the error $e_2(k)$ is proportional to the number of elements that switch. Based on this observation modified mismatch shaping (MMS) [1] was proposed. Here the number of elements that switch was targeted to be constant and the static error $e_1(k)$ was first-order shaped. However, a hardware-expensive vector quantiser structure was used and problems with $e_3(k)$ were not tackled.

Basic idea: Suppose the following restriction is set on the selection signal $S_i(k)$: '$S_i(k)$ and $S_i(k-1)$ are never both 1'. Then it is possible to simplify $e_2(k)$ and $e_3(k)$ to:

$$\begin{aligned} e_2(k) &= \delta \cdot (D(k) + D(k-1)) \\ e_3(k) &= \sum_{i=1}^{N} \delta_i S_i(k) + \sum_{i=1}^{N} \delta_i S_i(k-1) \end{aligned} \quad (2)$$

Now $e_2(k)$ depends linearly on the input value $D(k)$. So, under this restriction switching imperfections no longer cause nonlinearity. Furthermore, (1) and (2) show that, when $S_i(k)$ is generated by any